Carbohydrate Polymers **5** (1985) 367–389

Thermal Behavior of Amylose–Lipid Complexes

C.G. Biliaderis, C.M. Page, L. Slade* and R.R. Sirett

General Foods Inc., Research Department, Cobourg, Ontario, Canada K9A 4L4

(Received: 28 February 1985)

SUMMARY

Melting and crystallization phenomena of amylose–lipid complexes, crystallized either from dilute solution or concentrated amylose 'melts' under various conditions, were studied using differential scanning calorimetry (DSC). The melting enthalpies (complex/H_2O: 0·1–0·5 w/w) of the solution-grown crystalline complexes were 20·4 ± 0·8 J g^{-1} for amylose-monopalmitin (AM-1-C16), 26·5 ± 1·5 J g^{-1} for amylose-lysolecithin (AM-lys/in) and 26·6 ± 1·6 J g^{-1} for amylose-lauric acid (AM-C12). While melting of the AM-lys/in complex showed a single transition for all concentrations studied, the melting behavior of the AM-1-C16 and the AM-C12 was rather complex at low or intermediate water contents. At a heating rate of 10°C min^{-1} two endothermic transitions with an intermediate exothermic peak were observed, indicative of non-equilibrium melting. A process of partial melting, followed by recrystallization and final melting, is suggested to explain such multiple-melting characteristics. These phenomena become less prominent with increasing water content; presumably due to the depression of the glass transition (T_g) and the melting temperatures (T_m). The annealing behavior of AM-1-C16 further suggested that the development of new structural order upon heating takes place primarily after partial melting of the initial crystalline structure. Overall, the DSC data are typical of those for semicrystalline polymers and consistent with a lamellar type of molecular organization in the crystalline regions of these materials.

INTRODUCTION

Amylose forms crystalline complexes, of the well known 'V' polymorph, with a variety of polar and non-polar organic compounds

* Present address: General Foods Corporation, Tarrytown, New York, 10591, USA.

Carbohydrate Polymers 0144-8617/85/$03.30 –

(Young, 1984). These complexes play an essential role in every process associated with the utilization of starch-containing materials. Thus, texture and structural stability of cereals and starch-based products are greatly influenced by the complex formation of linear starch components with various ligands (Krog & Lauridsen, 1976; Lund, 1984; Schuster & Adams, 1984).

Although the conformation of amylose in solution is still the subject of extensive investigation and speculation (Banks & Greenwood, 1972; Jordan *et al.*, 1978; Cesaro & Brant, 1981; Kitamura *et al.*, 1982, 1984) there seems little doubt that coil → helix transitions are induced upon addition of complexing agents in an aqueous amylose solution. It is the ability of these materials to satisfy the solvation requirements of the helical cavity that enables the polysaccharide chain to adopt a regular conformation where the ligand molecule resides within the helix (Banks & Greenwood, 1975). It follows that such stable amylose–ligand helices foster nucleation and subsequent precipitation of crystalline chain aggregates. As the helical space in V-amylose is too narrow to accommodate bulky groups, the polar groups of monoglycerides are not included in the helix (Lagendijk & Pennings, 1970; Carlson *et al.*, 1979).

The structural features of V-amylose have advanced mainly from X-ray diffraction studies (Mikus *et al.*, 1946; Rundle, 1947; Takeo *et al.*, 1973). However, despite the acknowledged helical character of these complexes, a complete description of their structural characteristics and properties as they form during processing of starch-containing food materials is a difficult task since they can exist in various states of aggregation.

Attempts to characterize amylose–lipid complexes have been made recently using differential scanning calorimetry (DSC). Thus, studies on starch gelatinization by DSC have revealed a reversible high temperature transition (110–120°C), well above the melting endotherm of starch crystallites, which was assigned to the melting of the amylose–lipid complex (Donovan & Mapes, 1980; Hoover & Hadziyev, 1981). Furthermore, in model systems where amylose was heated in the presence of palmitic acid, multiple transitions were seen upon successive heating–cooling cycles of the same sample (Kugimiya *et al.*, 1980; Bulpin *et al.*, 1982). However, to our knowledge, there is no information in the literature about the mechanism or the conditions that govern the crystallization and melting phenomena of the amylose–lipid complexes, particularly in concentrated starch systems.Therefore,

the aim of the present study was to provide further insight into the amylose–lipid interactions, using DSC, under various conditions (temperature–time protocols, moisture content, type of lipid, etc.) often employed during processing of starch-based food materials.

EXPERIMENTAL

Materials

Lysolecithin (lys/in) from egg yolk (Type I), lauric acid (C-12) and monopalmitin (l-C16) were products of Sigma Chem. Corp. (St Louis, Missouri, USA). Blue Dextran (molecular weight 2 000 000) was supplied by Pharmacia Ltd (Montreal, Quebec, Canada). All other reagents used were of analytical grade.

Preparation and characterization of the amylose

The amylose used in the present study was prepared from a purified (< 0·5% protein) faba bean starch according to the method of Montgomery & Senti (1964). The molecular characteristics of this material have been reported elsewhere (Biliaderis *et al.*, 1981) and are summarized in Table 1. Its purity and molecular weight distribution were examined by gel chromatography. The chromatographic conditions were essentially as those reported by Biliaderis (1982). Amylose (60 mg)

TABLE 1
Molecular Characteristics of Faba Bean Amylose[a]

Iodine affinity ($g\ I_2/(100\ g)^{-1}$)	[η] ($ml\ g^{-1}$)	$\overline{DP}$[b]	*β-Amylolysis* (%)	$\beta + P$[c] (%)
19·6	188	1400	85·6 ± 1·5[d]	103·2 ± 1·8[d]

[a] Adapted from Biliaderis *et al.* (1981).
[b] $\overline{DP} = 7{\cdot}4\ [\eta]$ (Cowie & Greenwood, 1957).
[c] Concurrent action of β-amylase and pullulanase.
[d] $n = 3$.

was dispersed at 4°C in 0·5 ml of 40% aqueous $HClO_4$ (perchloric acid) and diluted first with 5 ml NaOH (0·144% w/w) and then to 50 ml with distilled water. Aliquots of 5 ml were applied to a Sepharose 2B (Pharmacia Ltd, Montreal, Canada) column (2·6 × 64 cm) and eluted with water (4°C) by the ascending method at a flow rate of 18 ml h^{-1}.

Collected fractions (3 ml) were assayed for total carbohydrates by the phenol–sulphuric acid method (Dubois *et al.*, 1956) and λ_{max} of the iodine–polysaccharide complexes according to Bailey & Whelan (1961). Exclusion volume (V_0) and total volume (V_t) were determined by chromatography of Blue Dextran and glucose, respectively.

Preparation of inclusion complexes

Three complexes with lys/in (AM-lys/in), lauric acid (AM-C12) and monopalmitin (AM-1-C16) were prepared. Faba bean amylose (400 mg) was first dissolved in 5 ml hot DMSO and then diluted with water at 100°C to a 0·8% (w/v) solution. Complexes were formed by adding a small volume of 3–5 ml of either aqueous (lys/in, 1-C16; maintained at 60°C) or methanolic (C-12) solution of the ligand to the amylose solution under vigorous stirring at 85°C. The weight ratio of amylose to the added ligand was 5 : 1. This ratio was selected according to Krog (1971), who reported that the iodine affinity of amylose is reduced to zero at this level of complexing agent. After 2 h, the solutions were slowly cooled and allowed to stand at room temperature for 3 days. The complexes were then recovered by centrifugation (8000 *g*), washed with water and/or chloroform to remove excess of the free ligand and dried under vacuum at 45°C for 48 h.

Differential scanning calorimetry (DSC)

The DSC studies were carried out using a DuPont 1090 Thermal Analyzer equipped with a pressure DSC cell. The cell base was operated at 10× sensitivity and calibrated with indium. The reproducibility of transition temperatures was generally ±0·3°C. Pressure of 1400 KPa (200 psi) with N_2 was used for all calorimetric experiments to eliminate the problem of pan failure due to moisture loss at temperatures above 120°C. Total sample weight was 7–12 mg and Ottawa sand was used as an inert material (reference pan) to balance the heat capacity of the sample pan. The thermal contact between the pan and the constantan

disc of the DSC cell was improved by using a small amount of a silicon heat sink compound (Dow Corning, Midland, Michigan, USA). All samples were prepared in DuPont coated aluminium pans by adding excess of deionized water to a pre-weighed dry sample of the complex (1–6 mg) and allowing for the water to evaporate until the desired moisture content was achieved. The sample was then compacted (only when water content $< 40\%$) with the plunger ram of the pan crimper and hermetically sealed. The samples of low moisture content ($< 60\%$) were kept overnight at room temperature to allow for better moisture equilibrium. These pans were re-weighed before the DSC experiment to ensure that water loss did not occur during storage. Data were recorded at 0·4 s intervals during the DSC run and stored on floppy disks. Data analysis was performed using the DuPont software analysis programs. To facilitate comparisons between thermal curves some of the data files were normalized to a constant sample weight.

Crystallization of amylose–lipid complexes in the presence of various amounts of water was also carried out in the DSC. Thus, after melting the complexes at 175°C for 10 min the samples were cooled to room temperature at a specified cooling rate. A container with liquid N_2 placed on top of the DSC cell was used to facilitate program cooling at a constant rate. The complexes generated by this method are called 'melt crystallized' to distinguish them from the original 'solution grown' complexes.

RESULTS AND DISCUSSION

Background

At this point it is useful to review some of the factors that can influence the crystallization and melting phenomena of polymers as well as how these processes are manifested in a DSC thermal curve. A typical three-step crystallization mechanism for semi-crystalline polymers involves: (a) nucleation (initiation of oriented chain segments); (b) propagation (crystal growth); and (c) maturation (crystal perfection and/or continued growth) (Wunderlich, 1976).

Chain folding is widely accepted as a common feature of polymer crystallization (Bovey, 1979). A sufficiently regular, flexible polymer will always crystallize from the random disordered state to a chain-

folded macroconformation. This process is mainly governed by the degree of supercooling (ΔT); the higher the ΔT the smaller the lamella thickness (Wunderlich, 1973; Shalaby, 1981). In dilute polymer solutions, although the conditions favor the growth of good crystals (i.e. interactions between molecules are minimal), there is in fact very little perfection, due to the chain folding. The regularity of the folds and the fold surfaces are dependent on the crystallization conditions as well as the structural regularity, the flexibility and the size of the molecule. Crystalline lamellae in a given sample of polymer have distinct melting points determined by their dimensions; small crystallites melt at lower temperatures. Since chain-folded crystals are not generally in thermodynamic equilibrium, they tend to show increased perfection upon heating (i.e. annealing) at temperatures below the melting point. Annealing of semicrystalline polymers may proceed with or without change in the lamella fold-length. Three different regions are recognized as far as the events that may take place during annealing (Wunderlich, 1976): (a) a low temperature region where changes in crystal defects occur without an increase in lamella thickness; (b) an intermediate temperature region where fold increase (thickening) happens without melting; and (c) a high temperature region where melting is followed by folded chain recrystallization. If annealing is carried out in the presence of a solvent, two additional effects can further influence the process: first, swelling and/or plasticization of the amorphous regions (glass transition, T_g, is depressed) which can affect chain mobility and thus the lamella thickening process in the crystallites; secondly, the melting point depression by the diluent which follows the Flory–Huggins equation (Flory, 1953) under equilibrium melting.

In studying polymeric materials by DSC one must also be aware of factors that can complicate the melting behavior of a specimen. The thermal curve of any semicrystalline material is in fact a composite product of two competing processes: (a) melting of the sample, according to the type and distribution of its crystallites; and (b) reorganization as it is heated during the scan. A common technique used to detect if the polymer is prone to annealing is to carry out the thermal analysis at various heating rates. Thus, for polymers that exhibit a single melting endotherm but whose behavior is complicated by lamella thickening, increasing the heating rate will decrease the observed melting temperature, since the lamellae are given less time to reorganize. This argument assumes, however, that neither low polymer

thermal conductivity nor superheating is complicating the observed behaviour. Multiple endotherms (usually two) have been also observed in thermal curves of semicrystalline polymers, which are often believed to be the result of melting, followed by recrystallization and final melting (Runt & Harrison, 1980; Wunderlich, 1980; Shalaby, 1981). If the high temperature endotherm is associated with the melting of reorganized material, one would expect its magnitude to decrease with increasing heating rate. Multiple peaks may also arise when the sample contains crystals of different thermal stability. In the latter case, however, the relative proportions of the transitions should remain unchanged under various heating rates.

Melting versus recrystallization phenomena

The thermal profiles of AM-lys/in and AM-1-C16 at 20% and 50% w/w (in water), respectively, are shown in Fig. 1. The complex formation was demonstrated to be reversible in all cases. Thus, a sharp exotherm was apparent on the cooling curves of the melted complexes, indicative of the crystallization. This transition displayed marked hysteresis (ΔT, 16–26°C; cooling rate 3–10°C min^{-1}) as one would anticipate considering that the process is nucleation controlled. The need for nucleation, followed by crystal growth, results in a temperature region of no crystallization below the melting temperature. Similar hysteresis phenomena have been reported for the thermally induced order → disorder transitions of carrageenan and agarose gel systems (Liang *et al.*, 1979; Morris *et al.*, 1980), which were interpreted as reflecting aggregation processes of the ordered polysaccharide chains. It appears, therefore, that the thermal events seen in the cooling curves are associated with the organization of the amylose-lipid helices into a supramolecular semicrystalline structure. Such molecular aggregates formed upon cooling may subsequently exhibit increasing perfection in their crystalline domains during the cooling cycle. In fact, a broad trailing shoulder was often seen on the cooling curves following the main crystallization peak, which can account for such processes occurring at a much slower rate.

In general, after the first heating, the recrystallized complexes (complex/H_2O: 0·1–0·4 w/w) showed a broader melting transition upon reheating. The melting enthalpies were also found between 70–87% for AM-1-C16, 71–87% for AM-lys/in and 66–71% for AM-C12 of those for

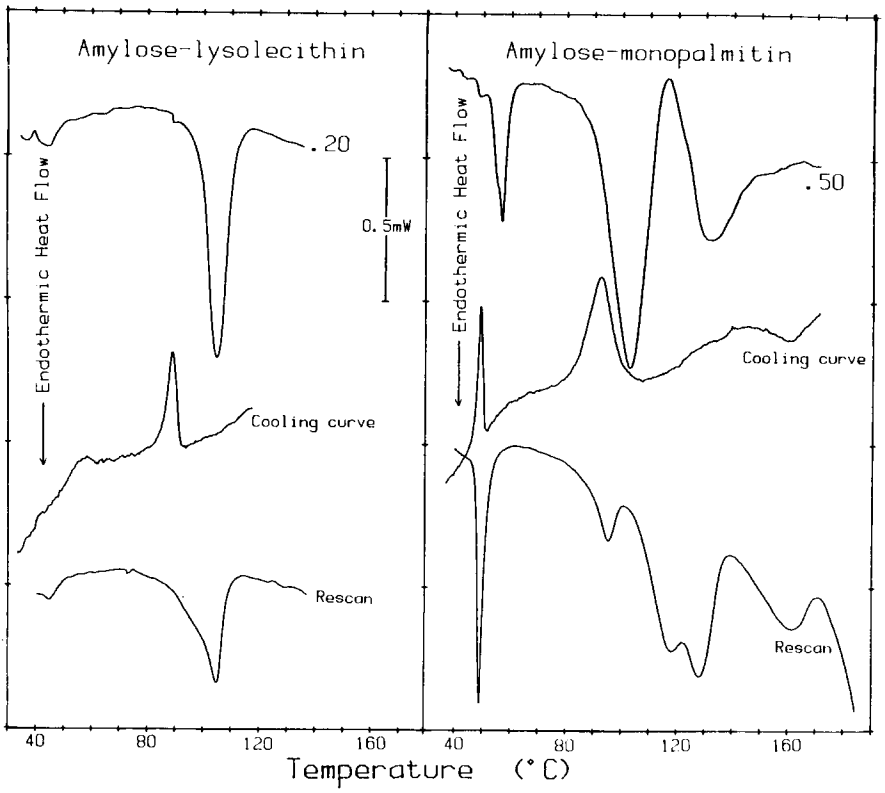

Fig. 1. DSC thermal curves of amylose-lysolecithin (20% w/w in H_2O) and amylose-monopalmitin (50% w/w in H_2O). Weight of complex (mg): AM-lys/in, 1·65; AM-1-C16, 5·00. Heating rate 10°C min^{-1}, cooling rate 5°C min^{-1}.

the solution-grown counterparts. These differences suggest that lower degrees of crystallinity and a wider range of crystallite distributions are obtained when molecular mobility is reduced; in concentrated solutions intermolecular types of interactions are favored.

Figure 2 illustrates the DSC melting curves of the three complexes, heated at 50% water content. The low temperature transitions correspond to the non-complexed lipid material (1-C16 57°C, C-12 42°C and lys/in 46°C). The amounts of these residual lipid fractions were less than 4% in all cases, based on their heat of fusion. While a single melting peak appeared for the AM-lys/in, it was interesting to observe two endothermic transitions for the AM-C12 and AM-1-C16. The

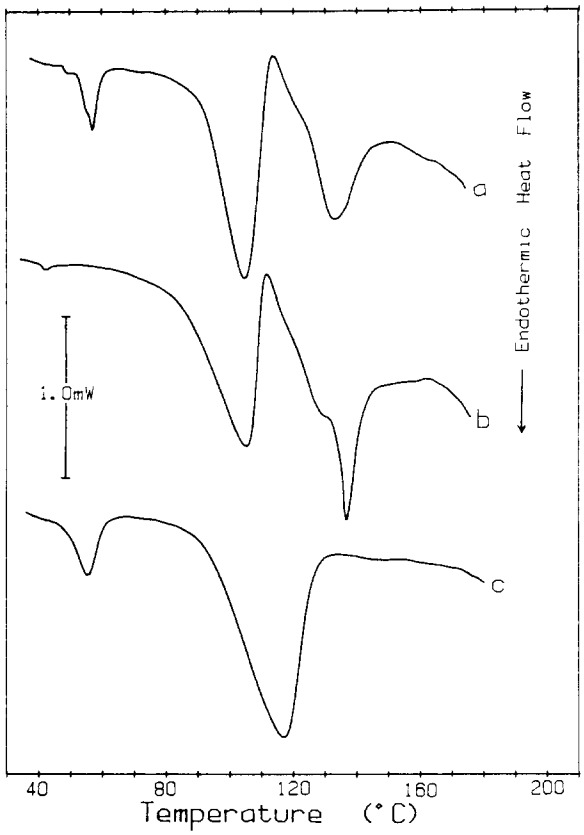

Fig. 2. DSC thermal curves of (50% w/w in H_2O) (a) AM-1-C16, (b) AM-C12 and (c) AM-lys/in. Weight of complex (mg): (a) 5·55; (b) 5·25; (c) 5·66. Heating rate 10°C min^{-1}.

apparently bimodal melting profile of these two complexes suggested either heterogeneity or recrystallization during the course of the DSC scan. Taking into account the uniform, although far from monodisperse, molecular weight distribution of the amylose (Fig. 3), it seems implausible that two distinct amylose chain populations are involved. On the other hand, the exothermic effect observed between the two melting transitions strongly suggests that recrystallization occurs after the initial melt. To further test this hypothesis, the melting behavior of these samples (at 50% w/w) was examined as a function of heating rate. Accordingly, for the AM-1-C16 complex, it was found that by

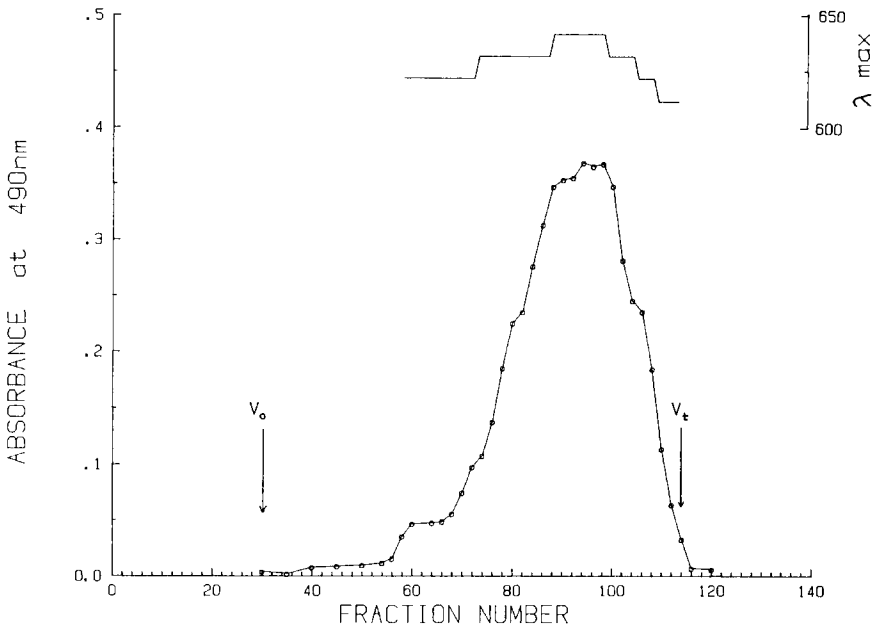

Fig. 3. Molecular weight distribution of faba bean amylose on a Sepharose 2B column (2·6 x 64 cm; flow rate 18 ml h^{-1}).

increasing the heating rate from 3°C min^{-1} to 40°C min^{-1} there was a progressive reduction in the magnitude of the high temperature transition (Fig. 4). In fact, at the fastest heating rate employed, the second endotherm was completely eliminated. These results suggest that only the first endotherm reflects the melting of the initial crystallites and that the second transition is a result of changes in the metastability of this system. At slow heating rates, even the first endotherm is not solely representative of the initial crystallite distribution since it is a composite of the melting and the recrystallization. Although AM-C12 exhibited similar trends in the thermal profiles over the same range of heating rates, it was observed that the second endotherm was still evident even at a heating rate of 40°C min^{-1}. This implies that AM-C12 is more inclined to reorganization upon heating than AM-1-C16. On the other hand, AM-lys/in showed no evidence for such processes (Fig. 5). A single endotherm was observed at all heating rates with a slight shift of the peak temperature from 117°C (at 3°C min^{-1}) to

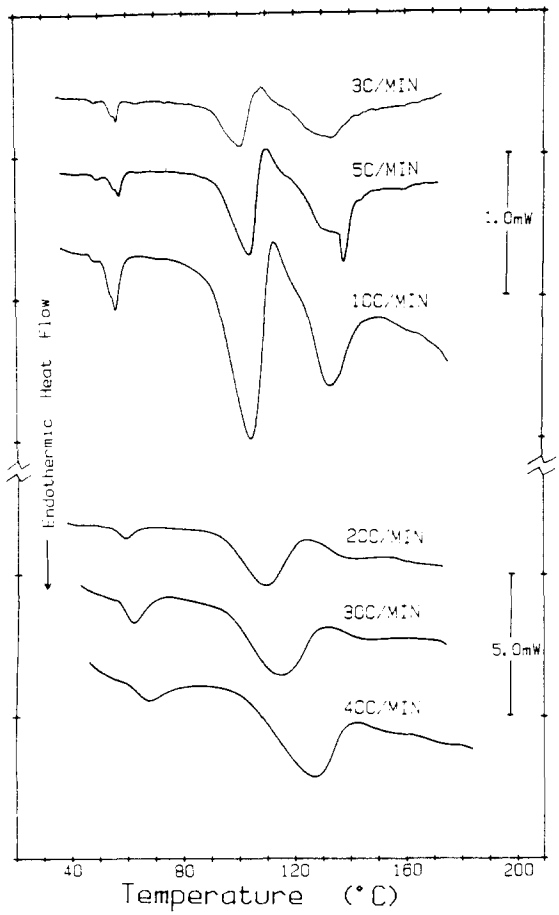

Fig. 4. DSC thermal curves of AM-1-C16 (50% w/w in H_2O) at different heating rates. Weight of complex form top to bottom (mg): 5·38, 5·60, 5·55, 4·72, 5·03 and 5·52.

121°C (at 40°C min^{-1}). The latter suggests that crystallite perfection via annealing without premelting of these materials is less likely.

Effects of water content on the melting behavior of amylose-lipid complexes

The thermal curves of the AM-1-C16 complex heated in the presence of various amounts of water (30–90%) are shown in Fig. 6, while the

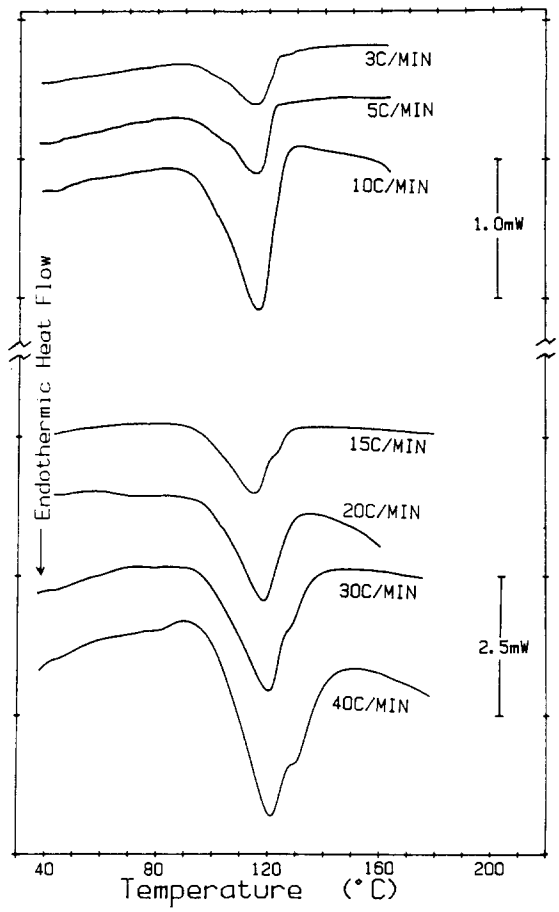

Fig. 5. DSC thermal curves of AM-lys/in (50% w/w in H_2O) at different heating rates. Weight of complex from top to bottom (mg): 4·08, 3·57, 4·04, 3·33, 3·27, 3·38 and 3·50.

effects of water content on the melting peak temperatures (first transition, T_m) and ΔH for these complexes are summarized in Figs 7 and 8, respectively.

At water concentrations higher than 80%, a single symmetrical endotherm was shown for all three complexes, indicating that melting becomes more highly cooperative in such systems (Fig. 6). Furthermore, from Fig. 7, it is apparent that the melting peak temperatures (T_m) remain constant at high water levels. The observed T_m values

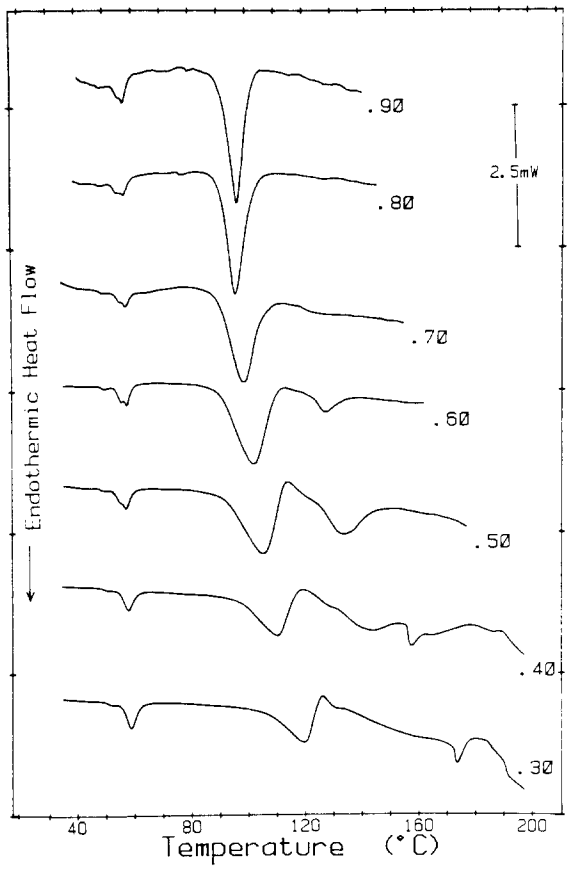

Fig. 6. DSC thermal curves of AM-1-C16 at various water contents (90 to 30%). Weight of complex from top to bottom (mg): 1·01, 2·01, 2·44, 2·64, 5·55, 4·35 and 4·21. Heating rate 10°C min^{-1}. All data files were normalized to a constant sample weight of 5·00 mg.

were 96, 97 and 104°C for AM-C12, AM-1-C16 and AM-lys/in, respectively. The melting temperature of AM-lys/in is in close agreement with the value of 105°C reported by Kugimiya & Donovan (1981). As the amount of water decreases, however, recrystallization superimposed on melting and secondary melting phenomena lead to a more complicated overall thermal behavior (Fig. 6). The exothermic effect observed after the first transition, as well as the progressive decrease in the magnitude of the melting endotherm, are evidence of recrystalliza-

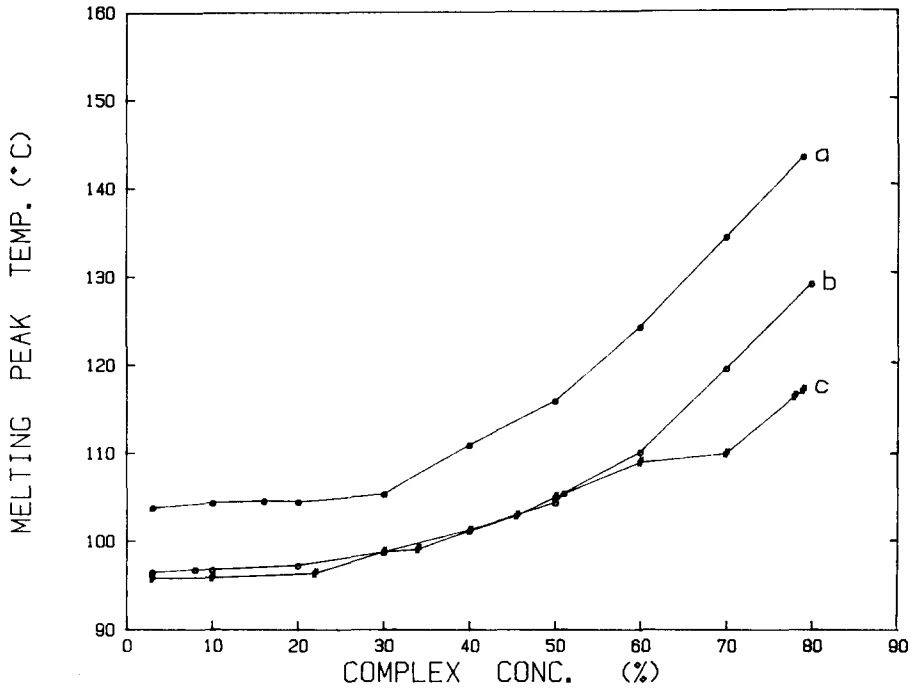

Fig. 7. Melting peak temperatures (°C) of (a) AM-lys/in, (b) AM-1-C16 and (c) AM-C12 as a function of complex concentration.

tion. Thus, water appears to play an essential role in controlling the rearrangement of the polysaccharide chains into new crystalline structures. Similar trends were also shown by AM-C12, while AM-lys/in exhibited single melting transitions for all levels of water concentration studied. The above behavior of AM-C12 and AM-1-C16 indicates that melting of these systems cannot be treated as an equilibrium or a zero-entropy production melting (i.e. a melting path where reorganization during heating is negligible).

At water contents below 70%, a progressive elevation of T_m was observed (Fig. 7). This can be best rationalized by considering both thermodynamic and non-thermodynamic effects. For the former, one would expect the well-known melting point depression with increasing amounts of water. Water which acts as a plasticizer of the amorphous regions (chain folds, loops and end segments) depresses both the glass transition (T_g) and the melting temperature (T_m) of

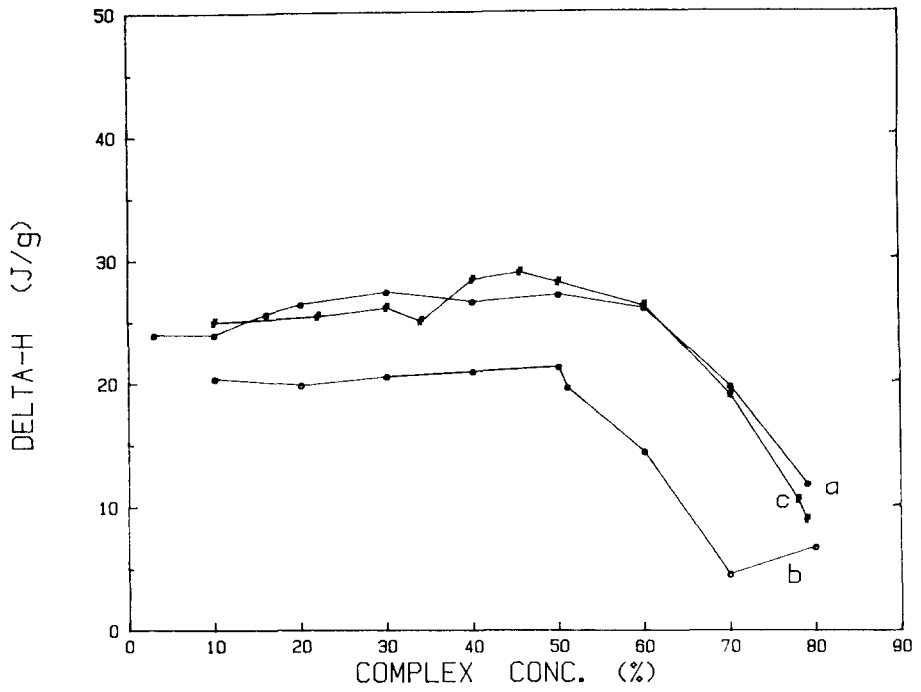

Fig. 8. Melting transition enthalpies (ΔH, J g^{-1}) of (a) AM-lys/in, (b) AM-1-C16 and (c) AM-C12 as a function of complex concentration.

synthetic (Bair, 1981) and natural semicrystalline polymers (Marshall & Petrie, 1980; Maurice *et al.*, 1985). In excess moisture situations (i.e. amorphous regions are fully plasticized) and at temperatures greater than T_g, the crystalline regions of these polymers will show much lower melting temperatures. Therefore, under these conditions the recrystallization phenomena become less prominent. For the non-thermodynamic contributions, structural changes in the sample due to recrystallization upon heating seem to be important, particularly for the AM-C12 and AM-1-C16 complexes. Electron and X-ray diffraction data on single crystals of V-amylose (Manley, 1964; Yamashita, 1965; Buleon *et al.*, 1984) provided evidence that the helical polysaccharide chains were folded having their chain axes perpendicular to the surface of the lamellae. The calculated long spacings, using the Bragg equation, indicated lamella thickness of 75 Å in one case (Manley, 1964) and 98 Å in the other (Yamashita, 1965) which would correspond to approxi-

mately 56 and 73 glucose units, respectively; calculations are based on the unit cell dimensions of Rundle (1947). Thus, taking into account the molecular size of the amylose used in this study ($\overline{DP}$, 1400; Table 1), it is reasonable to suggest that the amylose molecules in these complexes assume multiple chain folding within the same and/or successive lamellae. It is well known that macromolecular crystals with such large number of folds per molecule thicken rapidly during heating in the DSC. Lamella thickening results from migration of chain-ends and other amorphous chain segments through the crystal by longitudinal diffusion within the crystal lattice. It, therefore, implies significant molecular mobility along the direction of the chain axis and thus premelting is a prerequisite (Kovacs *et al.*, 1975; Point & Kovacs, 1980). In view of the above mechanism it seems plausible to suggest that similar phenomena take place during heating of AM-C12 and AM-1-C16 complexes.

The enthalpies of the melting transitions remain constant at water concentrations above 50% (Fig. 8). The estimated average values were: AM-lys/in, 26·5 ±1·5 J g^{-1} (n = 10); AM-C12, 26·6 ±1·6 J g^{-1} (n = 9); and AM-1-C16, 20·4 ±0·8 J g^{-1} (n = 7). Differences in the nucleation requirements and subsequent crystallite organization between these complexes may account for such differences in ΔH. Although further studies are required to understand these processes and their contribution to the enthalpy factor, one must point out that the observed ΔH values reflect the composite effect of several processes (crystallite melting, helix → coil transition, recrystallization phenomena, etc.). At water contents lower than 50%, the enthalpy of melting is significantly reduced (Fig. 8). It becomes difficult to assess accurately the enthalpy changes at such low moisture levels, if one considers the possibility of incomplete melting as well as the fact that processes with opposing thermal effect (melting vs. recrystallization) occur simultaneously.

Crystallization and melting as a function of water content, cooling mode and annealing treatments

Figure 9 illustrates the effect of complex concentration on the crystallization behavior of AM-1-C16 and AM-lys/in. The original thermal curves are presented along with the rescans after cooling the samples at 3°C min^{-1}. Although AM-lys/in showed no significant changes in the

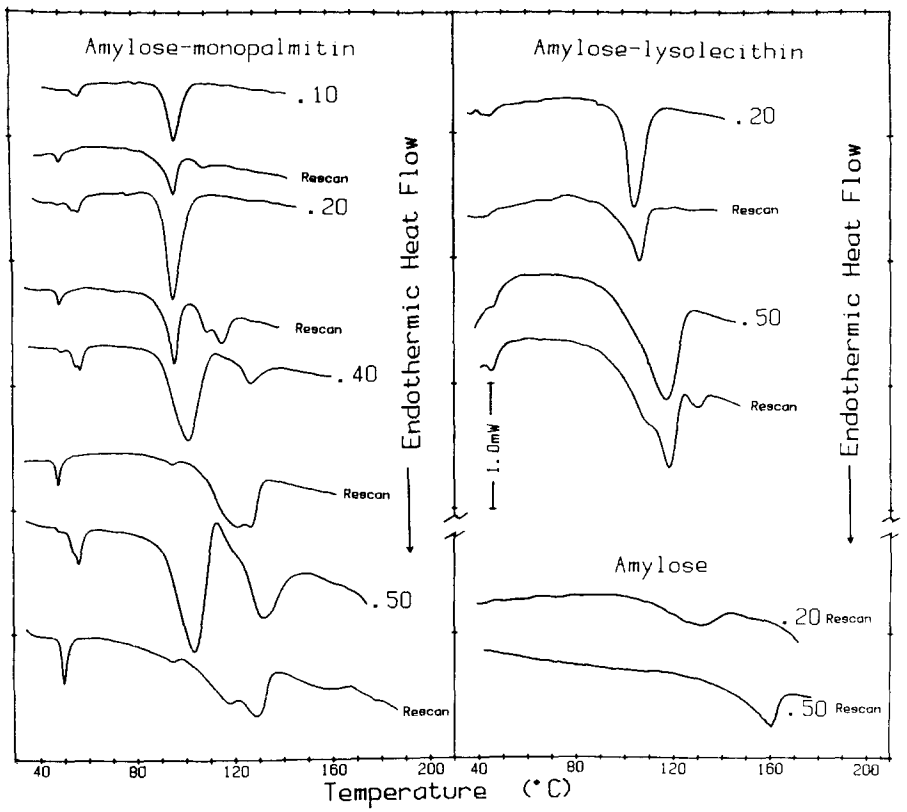

Fig. 9. Effect of the moisture content on the crystallization behavior of AM-1-C16, AM-lys/in and faba bean amylose cooled from the 'melt' at a constant cooling rate of 3°C min^{-1}; numbers designate the weight fraction of the solid material. Weight of solid material from top to bottom (mg): AM-1-C16, 1·01, 2·01, 2·65 and 4·17; AM-lys/in, 1·65 and 3·10; amylose, 2·23 and 4·40. Heating rate 10°C min^{-1}.

thermal profiles of the 'melt crystallized' complexes, AM-1-C16 formed new, more thermostable crystalline structures, particularly at low moisture contents. Increasing amounts of water, however, lower the melting peak temperature of the AM-1-C16, indicating that crystallites of intermediate and low perfection are formed during cooling; at 90% water content the typical thermal profile of the solution-grown metastable complex is obvious. We also found that, even in the presence of large amounts of water, it is possible to obtain complexes of higher

thermal stability by isothermal crystallization at temperatures above the melting point of the initial sample.

Alternatively, the thermal stability of the melt crystallized complexes can be controlled by monitoring the cooling rate. Thus, when samples of 50% AM-1-C16, AM-C12 and AM-lys/in were melted and then subjected to several cooling rates, polycrystalline structures of different thermal profiles were obtained. The thermal curves for the AM-1-C16 samples are presented in Fig. 10. Crystallization under slow cooling facilitates better organization of the polymer chains and thus results in crystalline structures of higher melting temperatures, presumably due to larger lamella thicknesses. It was also found that, in addition to the multiple melting transitions of these complexes, a small high temperature (150–160°C) endotherm was evident in the thermal curves of the melt crystallized samples. This transition may be associated with a structure formed by the uncomplexed amylose chains alone. Supporting evidence for this is provided by the fact that a single melting peak in the same temperature region was observed for similarly treated amylose samples (Fig. 10: h, i). While it is difficult to draw conclusions on the nature of the chain organization, it is reasonable to expect that, depending on the crystallization conditions, part of the amylose chains would not be involved in complex formation. These chains and/or chain segments could perhaps form structures of aggregated chains with high thermal stability. It is important further to note that the temperature of this transition is also dependent on the water content of the sample (Fig. 9).

The melting profiles of 50% AM-1-C16 complex annealed at different temperatures are presented in Fig. 11. Samples which were heated for several hours at temperatures just before the onset of the first melting transition exhibited very little reorganization (Fig. 11: b). However, as the annealing temperature increased from 80 to 95°C, there was a progressive reduction in the size of the low temperature melting peak as well as of the recrystallization exotherm. These observations provide additional evidence that reorganization of these complexes takes place predominantly after melting. It was also interesting to observe that, regardless of the temperature at which annealing was carried out, the transition temperature of the reorganized complex was constant at 130–135°C. This suggests that after melting a certain mode of crystallite reorganization is always preferred. Finally, when a specimen was heated up to 110°C it did not show any residual crystalline structure character-

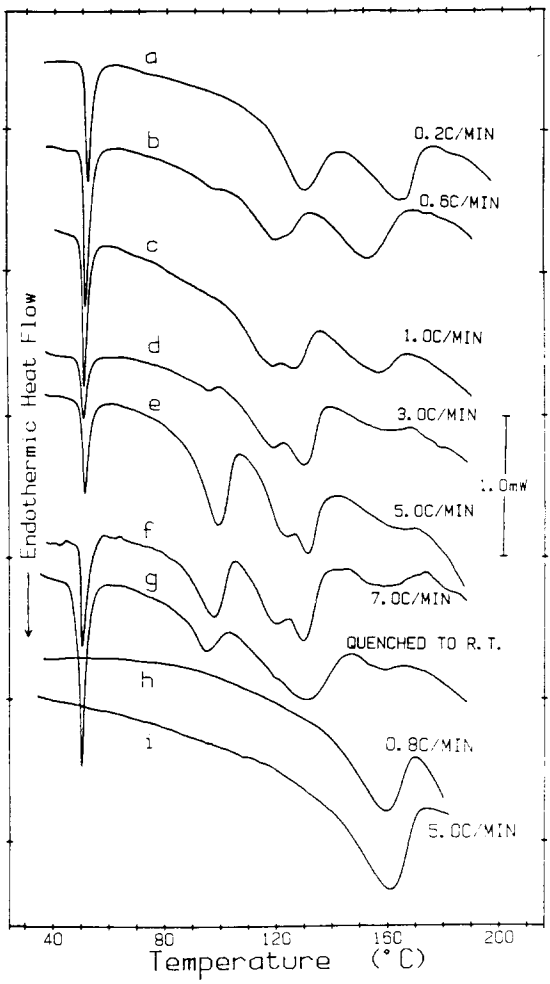

Fig. 10. Effect of the cooling rate on the crystallization behavior of 50% (w/w H_2O) AM-1-C16 complex ((a)-(g)) and faba bean amylose ((h), (i)). Samples were melted at 175°C for 10 min and then cooled to room temperature at the specified cooling rate. The recorded DSC thermal curves are those obtained on reheating at 10°C min^{-1}. Weight of solid materials (mg): (a) 5·00; (b) 5·04; (c) 5·68; (d) 4·87; (e) 5·28; (f) 5·56; (g) (quenched to room temperature) 5·53; (h) 5·33; (i) 5·69.

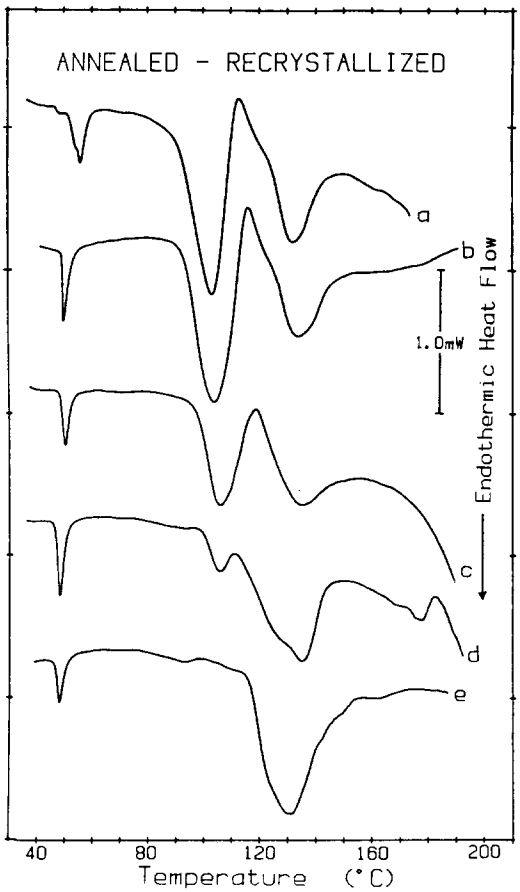

Fig. 11. Effect of different annealing treatments (temperature/time) on the thermal behavior of AM-1-C16 (50% w/w H_2O). Thermal treatments and weights of complex (mg): (a) control (non-treated), 5·55; (b) 80°C/2 h, 5·17; (c) 90°C/2 h, 5·34; (d) 95°C/2 h, 4·92; and (e) 110°C/2 h, 5·34. Heating rate 10°C min^{-1}.

istic of the initial sample (Fig. 11: e). Instead, the melting profile is exclusively attributed to the reorganized (perfected) material.

CONCLUSIONS

The melting behavior of the solution-grown crystalline amylose-lipid complexes was found to be dependent on the water content. At high

moisture levels, melting was highly cooperative and thus a single endothermic transition was shown at 96, 97 and 104°C for the AM-C12, AM-1-C16 and AM-lys/in, respectively.

Although AM-lys/in always exhibited a single transition, two melting endotherms, separated by an exothermic peak, were observed for AM-1-C16 and AM-C12 heated at intermediate or low water contents. This behavior is indicative of non-equilibrium melting of a metastable solid material. Evidence was provided that the thermal profiles of these complexes represent the composite thermal effect of two opposing processes: melting of the original crystallites and recrystallization during heating. The possibility of changes in lamella thickness as a result of such structural transformations is further suggested to account for the increase in melting temperature of the recrystallized material.

For these complexes, the use of non-equilibrium melting points with expressions such as the Flory–Huggins equation (describes only equilibrium melting) to investigate polymer–diluent interactions and determine equilibrium melting points (T_m°) is not appropriate.

The role of water is essential for both melting and crystallization phenomena of the amylose–lipid complexes. Water plasticizes the amorphous chain segments and thus facilitates greater chain mobility and subsequent melting of the crystallites at lower temperatures. Furthermore, crystallization at high water contents leads to metastable, less perfected, crystalline complexes.

The thermal profiles of the 'melt-crystallized' complexes showed lower transition enthalpies and had a wider distribution of crystalline components than their solution-grown counterparts. For these samples, a high temperature transition, above those attributed to the amylose–lipid complexes, was assigned to the disorganization of non-complexed aggregated amylose chains. The thermal stability of 'melt-crystallized' complexes can be controlled by monitoring the cooling rate and/or isothemal crystallization in conjunction with the water content of the system.

ACKNOWLEDGEMENTS

We would like to thank Dr Harry Levine and Terry Maurice for reviewing this paper.

REFERENCES

Bailey, J. M. & Whelan, W. J. (1961). *J. Biol. Chem.* **236**, 969.
Bair, H. E. (1981). In *Thermal characterization of polymeric materials*, ed. E. A. Turi, New York, Academic Press, p. 91.
Banks, W. & Greenwood, C. T. (1972). *Carbohydr. Res.* **21**, 229.
Banks, W. & Greenwood, C. T. (1975). *Starch and its components*, New York, Halsted Press.
Biliaderis, C. G. (1982). *Phytochemistry* **21**, 37.
Biliaderis, C. C., Grant, D. R. & Vose, J. R. (1981). *Cereal Chem.* **58**, 496.
Bovey, F. A. (1979). In *Macromolecules: An introduction to polymer science*, eds F. A. Bovey & F. H. Winslow, New York, Academic Press, p. 317.
Buleon, A., Duprat, F., Booy, F. P. & Chanzy, H. (1984). *Carbohydrate Polymers* **4**, 161.
Bulpin, P. V., Welsh, E. J. & Morris, E. R. (1982). *Starke* **34**, 335.
Carlson, T. L.-G., Larsson, D., Dinh-Nguyen, N. & Krog, N. (1979). *Starke* **31**, 222.
Cesaro, A. & Brant, D. (1981). In *Solution properties of polysaccharides*, ed. D. Brant, ACS Symposium Series 150, Washington, American Chemical Society, p. 513.
Cowie, J. M. G. & Greenwood, C. T. (1957). *J. Chem. Soc.* 2862.
Donovan, J. W. & Mapes, C. J. (1980). *Starke* **32**, 190.
Dubois, M., Gilles, K. A., Hamilton, J. K., Rebers, P. A. & Smith, F. (1956). *Analyt. Chem.* **28**, 350.
Flory, P. J. (1953). *Principles of polymer chemistry*, Ithaca, New York, Cornell University Press.
Hoover, R. & Hadziyev, D. (1981). *Starke* **33**, 390.
Jordan, R. C., Brant, D. & Cesaro, A. (1978). *Biopolymers* **17**, 2617.
Kitamura, S., Yunokawa, H. & Kuge, T. (1982). *Polymer J.* **14**, 85.
Kitamura, S., Tanahashi, H. & Kuge, T. (1984). *Biopolymers* **23**, 1043,
Kovacs, A. J., Gonthier, A. & Straupe, C. (1975). *J. Pol. Sci.* **C50**, 283.
Krog, N. (1971). *Starke* **23**, 206.
Krog, N. & Lauridsen. J. B. (1976). In *Food emulsions*, ed. S. Friberg, New York, Marcel Dekker, Inc., p. 127.
Kugimiya, M. & Donovan, J. W. (1981). *J. Food Sci.* **46**, 765.
Kugimiya, M., Donovan, J. W. & Wong, T. Y. (1980). *Starke* **32**, 265.
Lagendijk, J. & Pennings, H. J. (1970). *Cereal Science Today* **15**, 354.
Liang, J. N., Stevens, E. S., Morris, E. R. & Rees, D. A. (1979). *Biopolymers* **18**, 327.
Lund, D. (1984). *CRC Crit. Rev. Food Sci, Nutr.* **20**, 249.
Manley, R. S. J. (1964). *J. Polymer Sci.* **A2**, 4503.
Marshall, A. & Petrie, S. E. B. (1980). *J. Photogr. Sci.* **28**, 128.

Maurice, T. J., Slade, L., Sirett, R. R. & Page, C. M. (1985). In *Properties of water in foods*, eds D. Simatos & S. L. Mutton, The Netherlands, Nijhoff Dordrecht.

Mikus, F. F., Hixon, R. M. & Rundle, R. E. (1946). *J. Amer. Chem. Soc.* **68**, 1115.

Montgomery, E. M. & Senti, F. R. (1964). *J. Polymer Sci.* **28**, 1.

Morris, E. R., Rees, D. A., Norton, I. T. & Goodall, D. M. (1980). *Carbohydr. Res.* **80**, 317.

Point, J. J. & Kovacs, A. J. (1980). *Macromolecules* **13**, 399.

Rundle, R. E. (1947). *J. Amer. Chem. Soc.* **69**, 1769.

Runt, J. & Harrison, I. R. (1980). In *Methods of experimental physics*, New York, Academic Press, Chapter 9, p. 287.

Schuster, G. & Adams, W. F. (1984). In *Advances in cereal science & technology*, Vol. 6, ed. Y. Pomeranz, St Paul, Minnesota, Amer. Assoc. of Cereal Chemists, p. 139.

Shalaby, S. W. (1981). In *Thermal characterization of polymeric materials*, ed. E. A. Turi, New York, Academic Press, p. 235.

Takeo, K., Tokomura, A. & Kuge, T. (1973). *Starke* **25**, 357.

Wunderlich, B. (1973). *Macromolecular physics*, Vol. 1, New York, Academic Press.

Wunderlich, B. (1976). *Macromolecular physics*, Vol. 2, New York, Academic Press.

Wunderlich, B. (1980). *Macromolecular physics*, Vol. 3, New York, Academic Press.

Yamashita, Y. (1965). *J. Polymer Sci.* **A3**, 3251.

Young, A. H (1984). In *Starch chemistry and technology*, eds R. L. Whistler, J. N. BeMiller & E. F. Paschall, 2nd edn, New York, Academic Press, p. 260.